Asia Oceania Journal of Nuclear Medicine & Biology
http://aojnmb.mums.ac.ir
AOJNMB

^{18}F-THK 5351 and ^{11}C-PiB PET of the Thai normal brain template

Chanisa Chotipanich*, Supaporn Kongthai, Anchisa Kunawudhi, Chetsadaporn Promteangtrong, Attapon Jantarato

National Cyclotron and PET Centre, Chulabhorn Hospital, Chulabhorn Royal Academy, Bangkok, Thailand

ARTICLEINFO

Article type:
Original Article

Article history:
Received: 16 Jun 2020
Revised: 30 Jul 2020
Accepted: 28 Sep 2020

Keywords:
Brain template
Amyloid
Tau protein

ABSTRACT

Objective(s): The aim of the study was to create a local normal database brain template of Thai individuals for ^{11}C-Pittsburgh compound B (^{11}C-PiB) and ^{18}F-THK 5351 depositions using statistical parametric mapping (SPM) software, and to validate and optimize the established specific brain template for use in clinical practice with a highly reliability and reproducibility.

Methods: This prospective study was conducted in 24 healthy right-handed volunteers (13 men, 11 women; aged: 42–79 years) who underwent ^{18}F-THK 5351 and ^{11}C-PiB PET/CT scans. SPM was used for the ^{18}F-THK 5351 and ^{11}C-PiB PET/CT image analysis. All PET images were processed individually using Diffusion Tensor Image -Magnetic Resonance Imaging-weighted images (DTI-MRI images), which involved: (1) conversion of Digital Imaging and Communications in Medicine (DICOM) files into an analyzable file extension (.NIFTI) for statistical parametric mapping, (2) setting of the origin (the anterior commissure was used as the anatomical landmark), (3) re-alignment, (4) co-registration of PET with B0 (T1W) and DTI-MRI images, (5) normalization, and (6) normal verification using the Thai MRI standard. We then compared the normal PET template with the abnormal deposition area of different dementia syndromes, including Alzheimer's disease and progressive supranuclear palsy.

Results: This method was able to differentiate cognitively normal from Alzheimer's disease and progressive supranuclear palsy subjects .

Conclusions: This normal brain template was able to be integrated into clinical practice and research using PET analyses at our center.

Please cite this paper as:

Chotipanich Ch , Kongthai S, Kunawudhi A, Promteangtrong Ch, Jantarato A. ^{18}F-THK 5351 and ^{11}C-PiB PET of the Thai normal brain template. Asia Ocean J Nucl Med Biol. 2021; 9(1): 21-30. doi: 10.22038/AOJNMB.2020.49623.1338

Introduction

The accumulation of amyloid-β (Aβ) and hyperphosphorylated tau proteins are considered important biomarkers for Alzheimer's disease (AD) (1). AD is an important problem worldwide, and the dementia associated with AD can affect the quality of life of both patients and their families. Thus, it is critical to improve diagnosis and screening methods for early detection of AD (2).

Over the last decade, a number of radiopharmaceuticals for use with neuro positron emission tomography (PET) have been developed for in vivo detection of Aβ plaques and tau protein deposition. One of those tracers, ^{11}C-labeled Pittsburgh Compound-B (^{11}C-PiB), shows outstanding binding performance to amyloid plaque (3). Concurrently, ^{18}F-THK-5351 was developed and demonstrated highly selective binding to the tau protein (4). Both radiotracers are used for effective diagnosis of AD and other neurodegenerative diseases (5-6).

The neuro PET interpretation of amyloid and tau protein accumulation in the brain is based on both visual analysis and quantitative analysis by nuclear physicians. Both analysis methods can be used interchangeably for confirmation of each other. The improvement of qualitative analysis is important for increasing the accuracy and precision of diagnosis, particularly in complicated patients with uncertain accumulation of radiotracer. A technique for qualitative analysis involves comparison of data with a normal brain

* *Corresponding author:* Chanisa Chotipanich. National Cyclotron and PET Centre, Chulabhorn Hospital, Chulabhorn Royal Academy, 906 Kamphaeng Phet 6 Rd, Talat Bang Khen, Lak Si, Bangkok 10210, Thailand.Tel.: +662-574-3355 ext. 1211; E-mail: chanisa.cho@pccms.ac.th

template. This procedure can be applied with high reliability and allows detection of brain areas with abnormalities and radiotracer retention data. Brain template comparisons can be achieved with software such as the MIM neuro tool analysis, the Siemens Senium neuro database, and Cortex ID. However, the template establishment in those programs is based on a normal database of different populations. Thus, use of a specific local normal database can provide improved qualitative analysis of brain templates, with improved accuracy and precision of PET interpretation (7).

The aim of the present study was to create a local normal database brain template of Thai individuals for PiB and THK5351 depositions using statistical parametric mapping (SPM) software, and to validate and optimize the established specific brain template for use in clinical practice with a highly reliability and reproducibility.

Methods

This study was approved by the Human Research Ethics Committee of Chulabhorn Research Institute. Written informed consent was obtained from all participants before the study. All procedures performed in studies involving human participants were in accordance with the ethical standards of the institutional and/or national research committee and with the 1964 Helsinki declaration and its later amendments or comparable ethical standards.

Participants

Twenty-four right-handed volunteers (13 men, 11 women; age: 42-79 years; mean age: 59.67±10.84 years) with examinations from neurologists and neuropsychiatrists participated in this study. Cognitively normal criteria were defined as 1) mini-mental state examination (MMSE) of 24 of higher or score of more than 25 on the Montreal Cognitive Assessment (MoCA) 2) Clinical Dementia Rating (CDR) of 0, 3) preserved activities of daily living, 4) absence of significant levels of impairment in other cognitive domains, 5) no sign and symptom of mild cognitive impairment or dementia and 6) not diagnosed with probable AD by using criteria from the National Institute on Aging-Alzheimer's Association workgroups. All subjects had no concurrent underlying disease such as hypertension, dyslipidemia, diabetic mellitus, cardiovascular disease, pulmonary or renal condition. No participants had a history of psychological or neurological diseases, use of psychotropic drugs, or cancer found within the last 5 years. Magnetic resonance imaging (MRI) was performed in all participants. Structural MRI brain of each cognitively normal individuals showed no focal mass, acute infarction, intracranial hemorrhage, hydrocephalus, extra-axial collection or brain herniation .

Participant characteristics were shown in Table 1.

Table 1. Participant characteristics

Characteristics	
Sex (count, %)	
Male	13(54)
Female	11(46)
MoCA (score)	
Range	25-30
Mean	27.29±1.57
Median	27.5
Education, (year)	
Range	4-20
Mean	14.8±4.2
Median	16

Procedures

All participants underwent amyloid positron emission tomography with ^{11}C-PiB, and tau positron emission tomography with ^{18}F-THK 5351, using a Siemens/Biograph 16 scanner (Siemens Healthcare GmbH, Henkestr. 127, 91052 Erlangen, Germany) in three-dimensional (3D) mode within 2 weeks of a scan.

^{11}C-PiB acquisition procedure

All participants were scanned using a Siemens/Biograph 16 scanner in 3D mode. Dynamic imaging was then performed immediately after intravenous injection of 555 MBq (15 mCi) ^{11}C-PiB. A dynamic brain PET/computed tomography (CT) scan was obtained for 70 min, with brain CT images for

attenuation correction also collected. Image acquisition was performed using a matrix size=168, zoom=1, and a Gaussian filter with a full width at half-maximum of 5.0. Image reconstruction was performed into 7 frames, 10 min per frame, using the ordered subset expectation maximization with 4 iterations, 8 subsets, and a 4 mm pixel size. The iterative reconstruction images from 50 to 70 min were used for quantitative analysis.

^{18}F-THK 5351 acquisition procedure

Dynamic imaging was performed immediately after intravenous injection of 185 MBq (5 mCi) ^{18}F-THK 5351. A dynamic brain PET/CT scan was obtained for 90 min, with brain CT images for attenuation correction also collected. Image acquisition was performed using a matrix size=168, zoom=1, and a Gaussian filter with a full width at half-maximum of 5.0. Image reconstruction was performed into 4 frames, 20 min per frame, using the ordered subset expectation maximization with 4 iterations, 8 subsets, and a 4 mm pixel size. The iterative reconstruction images from 40 to 60 min were used for quantitative analysis .

The injected dose of ^{11}C-PiB and ^{18}F-THK 5351 for the whole body effective dose (ED) of each patient in our study was about 11.5 mSv.

MRI acquisition procedure

We acquired T1-MRI in all participants using a 3.0T MRI Siemens/Trio scanner (Siemens Healthcare GmbH, Henkestr. 127, 91052 Erlangen, Germany). The parameters used for the 3D T1 images included a sagittal slice thickness of 1.0 mm over contiguous slices with 50% overlap, a TR (time to repetition) of 1600 ms, a TE (time to echo) of 2.03 ms, a flip angle of 9°, and a matrix size of 256×256 pixels, reconstructed to 480×480 pixels over a field of view of 240 mm .

Data analysis

1. Template reconstruction process

All the images files from the acquisition process were exported into DICOM, a standard file extension for exportation. First, data exported with DICOM were converted into an analyzable file extension (.NIFTI) using the MRI conversion software. Converted data were then loaded into SPM2 software (distributed under General Public License as published by the Free Software Foundation) running on MATLAB software version 7 (MathWorks, Natick, MA, USA) to start the generation process. For each subject, a single frame of a PET image and a diffusion tensor image (DTI) were selected for setting the origin site by visual analysis. In this step, the anterior commissure was used as an anatomical landmark to establish a reference point for image orientation, and then all image frames of each subject were applied and adjusted with the anatomical reference (origin point) for realignment to the standard brain position, which is suitable for the anatomical registration process. These steps put all PET images into the same orientation. Next, the B0 MRI data acquired from the image processing of all subjects' DTI images were used for co-registration with the summation of the realigned PET images. This co-registration of functional data with anatomical data provides an appropriate anatomical orientation for use as a brain template, and these fusion data are termed DTI-prop tract.

DTI-prop tract data were normalized to the value of each pixel with the standard DTI-prop tract acquired from normal Thai individuals (provided by the Advanced Diagnostic Imaging and Image-Guided Minimal Invasive Therapy Center, Ramathibodi Hospital, Faculty of Medicine, Mahidol University, Thailand) for optimization of our template with a reliable data set. After normalization, the complete brain template for each radiopharmaceutical was created.

2. Generated template testing

The normal brain template for Thai subjects was tested by comparing the template with patients diagnosed with an abnormal ^{18}F-THK 5351 or ^{11}C-PiB in known brain regions. The results are confirmed using clinical data, the nuclear medicine physicians report by visual analysis, and the quantitative analysis in the specific region. The process of generating the brain template for the Thai population is shown in Figures 1-3.

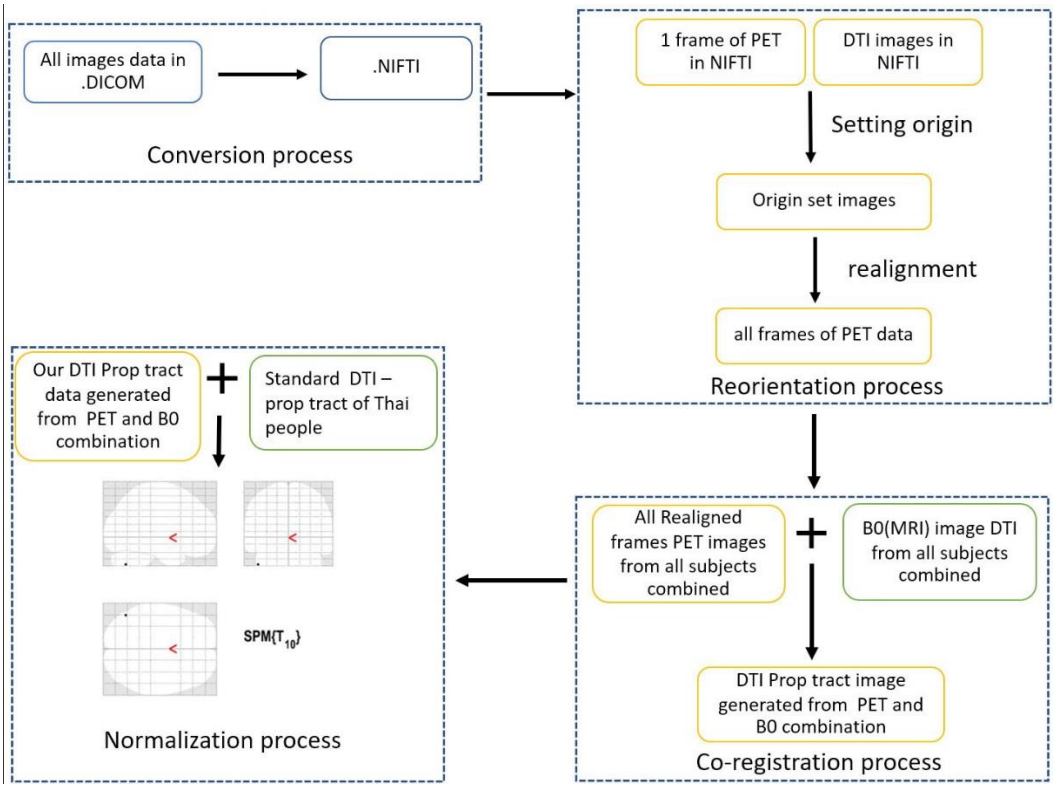

Figure 1. The process for generating the brain template for the Thai population. The analysis starts with conversion of DICOM files into NIFTI format, and then all data are analyzed in statistical parametric mapping (SPM) 2 using MATLAB 7 software. An origin point, as an appropriate reference landmark for image processing, is set in the PET and DTI images. This origin point is then applied to all frames of each subject for realignment of the data orientation. Next, a co-registration process is performed by applying B0 images acquired from all subjects' combined DTI data, and the DTI-prop tract data were then created. Finally, the standard DTI is used as the normalization data for completion of the brain template

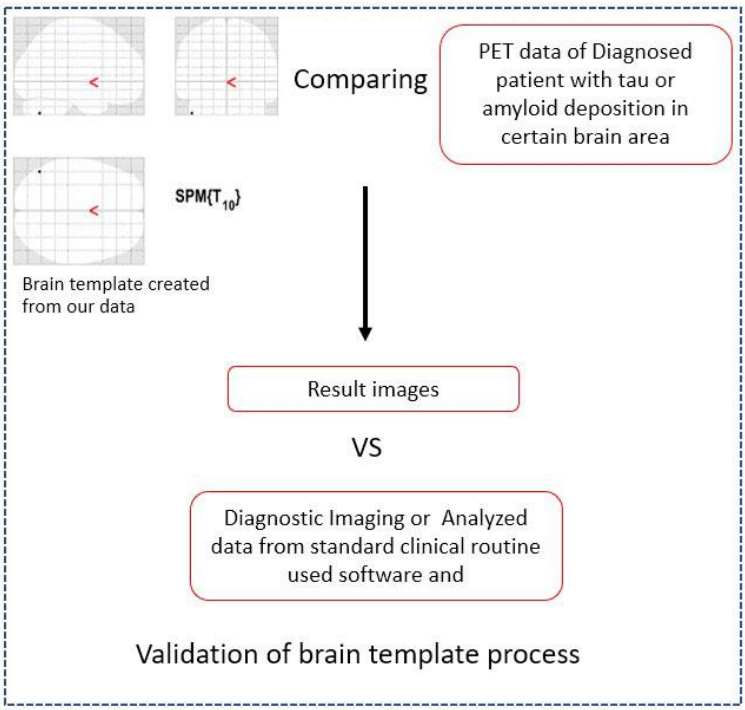

Figure 2. The validation process for the brain template from the Thai population database. The template was compared to a patient diagnosed with abnormal ^{18}F-THK 5351 or ^{11}C-PiB. The high intensity signal region in the brain represents an area of high accumulation of tau or amyloid. The correspondence was tested by comparing the result images with the standard method used in clinical diagnosis

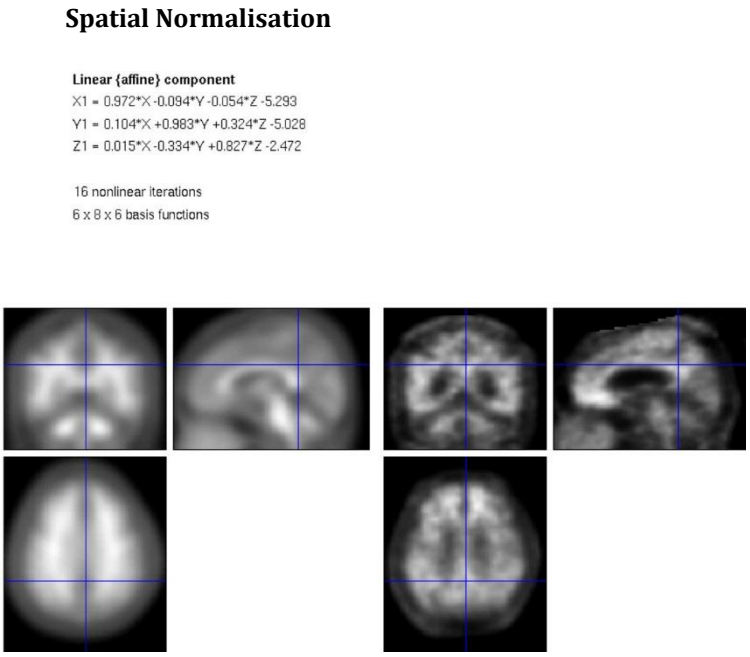

Figure 3. Imaging to verify normalization. The normal-PET brain template in the Thai population from each individual's head is compared to the anatomy of the normal-standard DTI of the Thai population. Left: normal-standard DTI in the Thai population. Right: normal-PET brain template in Thai population for each individual

Statistical analysis

Two sample t-test at 95 % confidence interval was applied for comparison between the generated brain template and the selected subjects, using SPM2 software (distributed under General Public License as published by the Free Software Foundation) running on MATLAB software version 7 (MathWorks, Natick, MA, USA).

Results

There was no statistically significant when comparing between men and women subjects with a good coefficient variation (CV) 18.16% of ranging age in all subjects .

The comparison of ^{11}C-PiB and ^{18}F-THK5351 data between normal healthy controls and early-onset AD (EOAD) and progressive supranuclear palsy (PSP) patients using a two-sample t-test showed accumulation of substances in the brain. The results are shown in Figures 4-6.

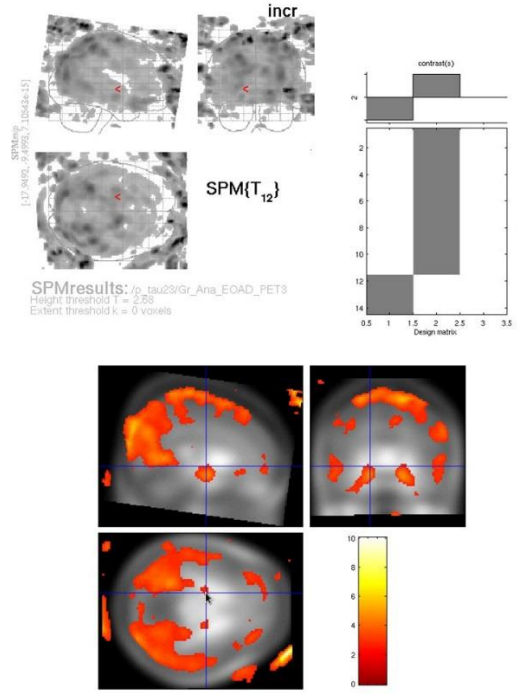

Figure 4. SPM analysis to compare between ^{18}F-THK 5351 in normal individuals and EOAD patients. There was higher accumulation in various brain areas in EOAD patients (two sample t-test; P=0.01), with different color shades showing a higher uptake of ^{18}F-THK 5351 than normal individuals in the frontal, parietal, occipital, and temporal regions

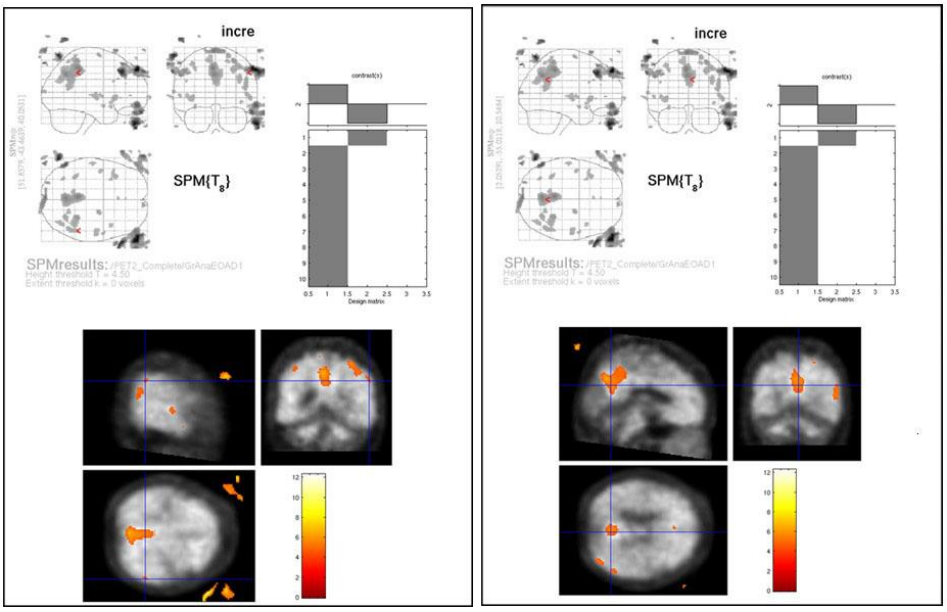

Figure 5. SPM analysis to compare between ^{11}C-PiB in normal individuals and EOAD patients. There was higher accumulation in various brain areas in EOAD patients (two sample t-test; P=0.001), with different color shades showing higher uptake of ^{11}C-PiB than normal individuals in the parietal and posterior cingulate regions

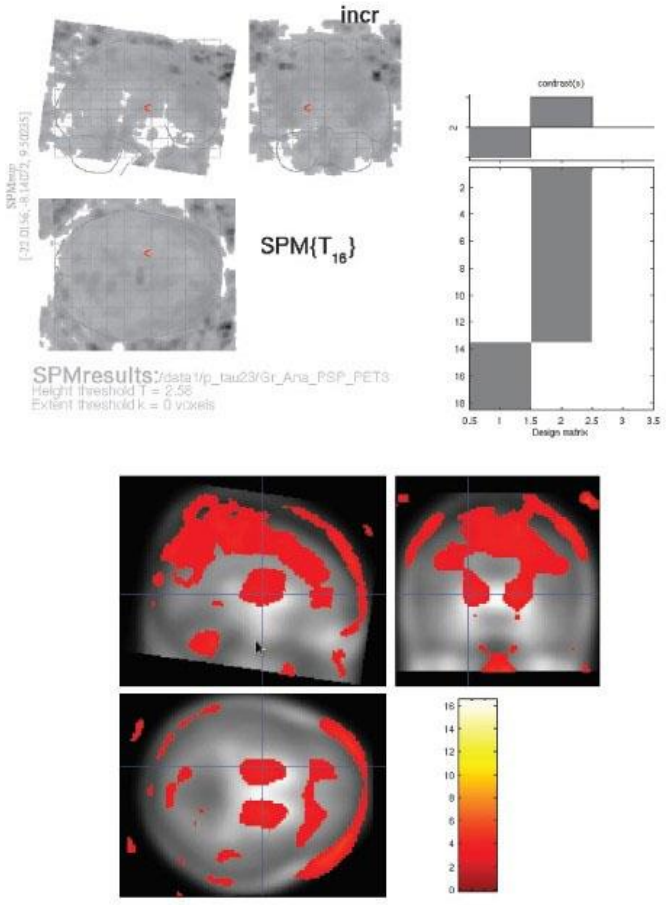

Figure 6. SPM analysis to compare between ^{18}F-THK 5351 in normal individuals and PSP patients. There was higher accumulation in various brain areas in PSP patients (two sample t-test; P=0.01), with different color shades showing higher uptake of ^{18}F-THK 5351 than normal individuals in the frontal, parietal, thalamus, caudate, and precuneus regions

The result of ^{11}C-PiB comparison between the normal brain template and the selected cases diagnosed with EOAD yielded higher uptake in the parietal and posterior cingulate regions.
Whereas, the result of ^{18}F-THK5351 demonstrated higher retention in selected cases diagnosed with EOAD compared with normal brain template, in various areas including frontal, parietal, occipital, and temporal regions. Similarly, there was also higher radiotracer uptake in the PSP patients at frontal, parietal, thalamus, caudate, and precuneus regions when compared with the normal brain template.

Discussion

Presently, quantitative and qualitative PET analysis is typically performed using a database of radiopharmaceutical uptake in brain regions from healthy subjects, which is set as a standard template for diagnosis of neurodegenerative diseases. Some commercial brain templates are available, although they may not appropriate for the Thai population, as different ethnicities can show anatomical and physiological differences in the brain (8,9). Thus, in the present study we created a normal brain template from PET images acquired from the cognitively normal Thai population. To develop this brain template, we obtained a database of radiopharmaceutical uptake in the brain using ^{18}F-THK-5351 and ^{11}C-PiB PET scans.

Registration of multi-modality images between PET and MRI is a fundamental task in 3D image analysis. While commercial brain templates used for interpretation of anatomical localization are based on the American or European populations, differences between races may influence the anatomical localization (9, 10). In the present study, the subjects were of Thai ethnicity, representing an Asian population. Asian body mass index values are generally lower than the American and European populations, which can result in spatial misregistration of images, and decrease the accuracy and precision of the interpretation .

Similarly, the physiological uptake of ^{18}F-THK-5351 and ^{11}C-PiB in the brain may differ according to ethnicity. Apolipoprotein E (APOE) is a genetic risk factor for developing AD. In healthy subjects, APOE e4 genotype was noted with high accumulation of ^{11}C-PiB (11-13).

Ward et al. reported that the highest estimates of the APOE e4 genotype were in Northern Europe, and the lowest in Asia and Southern Europe (12). Thus, our brain template represents the anatomy and physiology of the Thai population very well. The retention of Aβ and phosphorylated tau protein were also reported in the healthy brain. Thus, visual analysis may not provide the highest accuracy and precision for differential diagnosis or clinical screening because of contrast adjustment or physician experience, particularly in challenging cases with uncertain accumulation in a specific brain region or unclear uptake of radiotracer (14). Thus, the use of brain templates involving computerized analysis of the healthy brain was established for assisting physicians in these circumstances .

The validation process for the generated brain template involved a comparison between the template and selected patients with a final diagnosis by neurologists and neuropsychiatrists. For PiB retention in validated patients diagnosed with EOAD, the parietal and posterior cingulate regions showed marked increases in deposition. MRI studies have shown that involvement of those white matter regions is an important component of the clinical presentation of EOAD (15). Shinotoh et al. also reported accumulation of amyloid plaque in the lateral parietal cortices (+55%) and posterior cingulate (+43%) of an EOAD patient (16). In accordance with the validation result using THK5351 brain template, our selected validation case demonstrated higher deposition in a specific brain area related to the patient's clinical presentation. We also observed higher deposition in the frontal, parietal, occipital, and temporal regions compared with the normal brain template, similar to previous reports describing extensive and marked elevations in deposition of phosphorylated tau in the neocortex area (Bark stage V/VI) (17-19). Further, we performed THK5351 brain template validation using a selected case diagnosed with PSP. The comparison of THK5351 between the normal brain template and the selected case showed higher aggregation of radiotracer in the frontal, parietal, thalamic, caudate, and precuneus regions. Similar regions of tau accumulation were reported in a THK5351-PET study in the basal ganglia of PSP patients (20). Thus, our established brain template was reliable for comparing to real patients diagnosed with a neurological disease and may be applicable for use in clinical practice.

Our brain template calculated from a local Thai PET database of PiB and THK5351 accumulation was developed using MATLAB and SPM software, which are based on the combination of voxel-based morphometry and DTI for anatomical registration and normalization of PET data. These templates from our local database were validated using standard diagnosis, and showed highly accurate results using specific subjects for PET neuro analysis. Poussier et al. performed a quantitative analysis of rat brain images obtained from ^{18}F-FDG PET using a brain template model

based on block matching and voxel-based analyses for specific rat species, and developed an adaptive brain template for the detection of brain abnormalities (21). Nie et al. also demonstrated the utility of SPM for creation of a brain template in a rat brain model, which enhanced the detection potential of fluorodeoxyglucose (FDG) -PET functional images in rats with left side middle cerebral artery occlusion compared with normal controls (22). A local brain template developed from in-house software (SPM extension on MATLAB) was also applied clinically to examine age-related changes in FDG-PET images in 84 neurologically healthy subjects (23). In that study, age-related changes in brain FDG uptake were accurately determined by applying the SPM method of voxel-based quantitative analysis to a template that had precise characteristics of the subjects. Similarly, Della et al. reported that a population-specific FDG neuro template-based normalization in significant brain regions for various dementia subtypes, including mild cognitive impairment, probable AD, frontotemporal lobar degeneration, and dementia with Lewy bodies, provided highly accurate estimates of metabolic abnormalities and higher diagnostic performance (24).

Overall, these studies suggest that the use of brain templates can elevate the performance of both qualitative and quantitative studies for PET neuro examination, particularly when the template is constructed from a local database. Interestingly, the majority of recently reported brain templates have utilized ^{18}F-FDG accumulation, a commonly used radiotracer. By contrast, our study used PiB for Aβ deposition and THK5351 for phosphorylated tau deposition, which is considered a hallmark of various neurodegenerative diseases. This template may be useful clinically for screening or in combination with commercial brain template software such as MIM neuro-tool.

There are some potential limitations of our study. There was a small number of subjects, which prevented us from dividing our subjects into subgroup for the establishment of specific age match or sex match template. Whereas, the accuracy of our brain template should be improved in in future studies by increasing the population size. ^{18}F-THK 5351 tracer itself has limitation because ^{18}F-THK 5351 PET has off-target binding to monoamine oxidase-B (MAO-B) (25, 26). The tracer is known to accumulate not only neurofibrillary tangles but neurofibrillary tangles combining with reactive astrocytes. MAO-B distribution throughout the whole brain and subcortical structure should be concerned for tau PET interpretation. Nevertheless, we validated the use of this normal brain template in SPM software, as a prerequisite for statistical comparison of normal and neurodegenerative changes. Indeed, the brain regions with high deposition of ^{18}F-THK-5351 and ^{11}C-PiB were matched with abnormal regions in AD and PSP patients, which related to their clinical diagnosis. These data suggest that use of this template as a tool for a diagnostic tool is feasible.

Conclusion

This is the first report describing the Thai normal brain template. This normal brain template may be useful clinically in the Thai population by providing more effective discrimination between normal healthy patients and those with neurodegenerative diseases. Our normal brain template provides a higher degree of accuracy for ^{18}F-THK-5351 and ^{11}C-PiB imaging, as well as increased precision for anatomical registration of brain regions.

Acknowledgements

The authors thank Professor Shozo Furumoto, University of Tohoku, Sendai, Japan for providing the THK precursor, and Professor Eyal Mishani, Director of Cyclotron/Radiochemistry Unit, Department of Nuclear Medicine, Hadassah Medical Center, Israel for consulting with radiotracer production at our National Cyclotron and PET Centre, Chulabhorn Hospital, Chulabhorn Royal Academy, Bangkok, Thailand. Also, we acknowledge the help of Dr. Witaya Sungkarat, M.D., PhD. Advanced diagnostic imaging center (AIMC), Department of Radiology, Faculty of Medicine Ramathibodi hospital, Mahidol University, Bangkok, Thailand for imaging analysis. We also thank Edanz Group (https://en-author-services.edanzgroup.com/) for editing a draft of this manuscript .

Source of support: Chulabhorn Hospital Research Fund

References

1. Gulisano W, Maugeri D, Baltrons MA, Fà M, Amato A, Palmeri A, et al. Role of Amyloid-β and Tau Proteins in Alzheimer's disease: Confuting the Amyloid Cascade. J Alzheimers Dis. 2018; 64:S611–31.
2. GBD 2016 Dementia Collaborators. Global, regional, and national burden of Alzheimer's disease and other dementias, 1990-2016: a systematic analysis for the Global Burden of Disease Study 2016. Lancet Neurol. 2019; 18:88–106.
3. Zhang S, Smailagic N, Hyde C, Noel-Storr AH, Takwoingi Y, McShane R, et al. (11)C-PIB-PET for the early diagnosis of Alzheimer's disease

dementia and other dementias in people with mild cognitive impairment (MCI). Cochrane Database Syst Rev. 2014; 23:CD010386. doi: 10.1002/14651858.CD010386.
4. Harada R, Okamura N, Furumoto S, Furukawa K, Ishiki A, Tomita N, et al. [18F]THK-5117 PET for assessing neurofibrillary pathology in Alzheimer's disease. Eur J Nucl Med Mol Imaging. 2015; 20:42.
5. Okamura N, Harada R, Ishiki A, Kikuchi A, Nakamura T, Kudo Y. The development and validation of tau PET tracers: current status and future directions. Clin Transl Imaging. 2018; 6:305–16.
6. Quigley H, Colloby SJ, O'Brien JT. PET imaging of brain amyloid in dementia: a review. Int J Geriatr Psychiatry. 2011; 26:991–9.
7. Rao NP, Jeelani H, Achalia R, Achalia G, Jacob A, Bharath R dawn, et al. Population differences in brain morphology: Need for population specific brain template. Psychiatry Res. Neuroimaging. 2017; 265:1–8.
8. Duara R, Loewenstein DA, Lizarraga G, Adjouadi M, Barker WW, Greig-Custo MT, et al. Effect of age, ethnicity, sex, cognitive status and APOE genotype on amyloid load and the threshold for amyloid positivity. Neuroimage Clin. 2019; 22:101800. doi: 10.1016/j.nicl. 2019.101800.
9. Durbar U. Racial variations in different skulls. J Pharm Sci and Res. 2014; 6:370-2.
10. Wei L, Guo K, Li Y, Guo Z, Gao C, Yuan M, et al. Construction of a novel Chinese normal brain database using 18F-FDG PET images and MIMneuro software, the initial application in epilepsy. Int J Neurosci. 2018; 129:417-22.
11. Reiman EM, Chen K, Liu X, Bandy D, Yu M, Lee W, et al. Fibrillar amyloid- burden in cognitively normal people at 3 levels of genetic risk for Alzheimer's disease. Proc Natl Acad Sci USA. 2009; 106:6820-5.
12. Ward A, Crean S, Mercaldi CJ, Collins JM, Boyd D, Cook MN, et al. Prevalence of Apolipoprotein E4 Genotype and Homozygotes (APOE e4/4) among Patients Diagnosed with Alzheimer's Disease: A Systematic Review and Meta-Analysis. Neuroepidemiology. 2012; 38:1-17.
13. Reitz C, Mayeux R. Alzheimer disease: Epidemiology, diagnostic criteria, risk factors and biomarkers. Biochem Pharmacol. 2014; 88:640-51.
14. Sun FT, Schriber RA, Greenia JM, He J, Gitcho A, Jagust WJ. Automated Template-based PET Region of Interest Analyses in the Aging Brain. Neuroimage. 2007; 34:608–17.
15. Mendez MF. Early-Onset Alzheimer's Disease. Neurol Clin. 2017; 35:263–81.
16. Shinotoh H. IC-01-05: Mapping of amyloid deposition in early- and late-onset Alzheimer's disease. Alzheimers Dement. 2008; 4:T3–4. doi: 10.1016/j.jalz.2008.05.1153.
17. Okamura N, Harada R, Furumoto S, Arai H, Yanai K, Kudo Y. Tau PET Imaging in Alzheimer's Disease. Curr Neurol Neurosci Rep. 2014; 14:1–7.
18. Braak H, Braak E. Neuropathological staging of Alzheimer-related changes. Acta Neuropathol.1991; 82:239–59.
19. Schöll M, Maass A, Mattsson N, Ashton NJ, Blennow K, Zetterberg H, et al. Biomarkers for tau pathology. Mol Cell Neurosci. 2019; 97:18–33.
20. Alster P, Madetko NK, Koziorowski DM, Królicki L, Budrewicz S, Friedman A. Accumulation of Tau Protein, Metabolism and Perfusion-Application and Efficacy of Positron Emission Tomography (PET) and Single Photon Emission Computed Tomography (SPECT) Imaging in the Examination of Progressive Supranuclear Palsy (PSP) and Corticobasal Syndrome (CBS). Front Neurol. 2019; 10:101. doi: 10.3389/fneur.2019.00101.
21. Poussier S, Maskali F, Vexiau G, Verger A, Boutley H, Karcher G, et al. Quantitative SPM Analysis Involving an Adaptive Template May Be Easily Applied to [18F]FDG PET Images of the Rat Brain. Mol Imaging Biol. 2017; 19:731–5.
22. Nie B, Liu H, Chen K, Jiang X, Shan B. A Statistical Parametric Mapping Toolbox Used for Voxel-Wise Analysis of FDG-PET Images of Rat Brain. PLOS ONE. 2014; 9:e108295. doi: 10.1371/journal. pone.0108295.
23. Van Der Gucht A, Verger A, Guedj E, Malandain G, Hossu G, Yagdigul Y, et al. Age-related changes in FDG brain uptake are more accurately assessed when applying an adaptive template to the SPM method of voxel-based quantitative analysis. Ann Nucl Med. 2015; 29:921–8.
24. Della Rosa PA, Cerami C, Gallivanone F, Prestia A, Caroli A, Castiglioni I, et al. A standardized [18F]-FDG-PET template for spatial normalization in statistical parametric mapping of dementia. Neuroinformatics. 2014; 12:575–93.
25. Ng KP, Pascoal TA, Mathotaarachchi S, Therriault J, Kang MS, Shin M, et al. Monoamine oxidase B inhibitor, selegiline, reduces 18F-THK5351 uptake in the human brain. Alzheimers Res Ther. 2017; 9:25. doi: 10.118 6/s13195-017-0253-y.

26. Harada R, Ishiki A, Kai H, Sato N, Furukawa K, Furumoto S, et al. Correlations of ^{18}F-THK5351 PET with Postmortem Burden of Tau and Astrogliosis in Alzheimer Disease. J Nucl Med. 2018; 59:671-674.